RF DESIGN OF A HIGH-FREQUENCY RFQ LINAC FOR PIXE ANALYSIS*

H. W. Pommerenke[†,1,2], A. Bilton[1], A. Grudiev[1], A. M. Lombardi[1], S. Mathot[1],
E. Montesinos[1], M. Timmins[1], M. Vretenar[1], U. van Rienen[2]
[1] CERN, Geneva, Switzerland
[2] University of Rostock, Germany

Abstract

Protons with an energy of few MeV are commonly used for Ion Beam Analysis of materials, in particular with the Proton Induced X-ray Emission technique (PIXE). Because of its non-damaging character, PIXE is used in a variety of fields, in particular for the diagnosis of cultural heritage artwork. A compact accelerator based on a high frequency RFQ (Radio Frequency Quadrupole) linac has been designed and is being built at CERN. The length of the RFQ is only one meter and it allows the acceleration of a proton beam up to an energy of 2 MeV. The complete system is conceived to be transportable, allowing PIXE analysis almost anywhere. This paper covers the RF design of the compact RFQ operating at 750 MHz. We present general accelerator parameters and the current state of the RF design, which includes RFQ geometry and coupler design, thermal simulation and first particle tracking results.

INTRODUCTION

The Proton Induced X-Ray Emission (PIXE) [1] is a widely used method for cultural heritage material characterization (among others). It allows for a non-damaging and highly sensitive quantitative analysis by stimulating specimen atoms using 2 to 4 MeV proton beams and measuring the emitted X-ray spectrum.

Conventional electrostatic PIXE accelerators require significant space and infrastructure and are thus installed in dedicated centres. Contrarily, an RFQ operating at 750 MHz is able to provide 2 MeV protons over the length of just one meter, as proposed in [2]. The PIXE RFQ is developed within the context of the MACHINA project [3], whose aim is to build the first transportable system for *in situ* ion beam analysis. The RFQ design is based on the high-frequency RFQ for medical applications [2, 4, 5], adapted to the requirements of PIXE analysis. A selection of design parameters is presented in Table 1.

RF DESIGN

In general, all geometries are optimised to a resonant frequency of $f_0 = 749.48$ MHz, as well as minimum surface losses expressed by a maximum Q_0 factor. While a circular shape of the four quadrants would be the optimum in this

Table 1: Design Parameters of the PIXE RFQ

Input energy	$\mathcal{E}_\text{in}$	20	keV
Output energy	$\mathcal{E}_\text{out}$	2	MeV
RF frequency	f_0	749.48	MHz
RFQ length		1072.938	mm
Vane voltage	V	35	kV
Min. aperture		0.7	mm
Vane tip radius		1.439	mm
Peak current		200	nA
Transmission	T	30	%
Max. duty cycle	d_max	2.5	%

regard, a planar back side surface is used to simplify the machining (Fig. 1). The cavity geometries of the two RFQ modules are slightly different to account for the changing vane modulation.
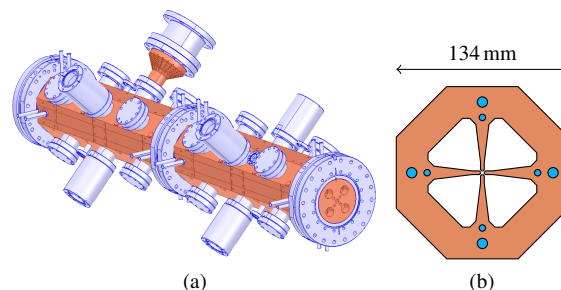

Figure 1: CAD model of the PIXE RFQ. (a) Accelerator with equipped tuners, pumping ports, and coupler. (b) 2D cavity cross section with water cooling channels.

The RFQ is terminated by two end plates with holes in each quadrant that allow for bead-pull measurement access. Further, four dipole stabilization rods on each end plate are used to give the maximum possible spectral margin of ± 12 MHz from the quadrupole operating mode (TE$_{210}$) to the next closest higher order modes (TE$_{211}$ and TE$_{111}$).

Figure 2 shows the surface electric field E_s at the vane tip. The overall maximum $E_\text{s} = 39.1$ MV/m occurs at the gap between the two RFQ modules (Fig. 2b). Excluding this effect, the maximum surface field is located in the bunching section of the RFQ with $E_\text{s} = 36.5$ MV/m (Fig. 2a).

The shapes of tuners and pumping ports are similarly optimised for minimum losses. The tuners are copper slugs with a conic tip (Fig. 3a). The pumping ports end with crossbars that help conducting the surface currents (Fig. 3b).

The total RF power P_0 dissipated through surface losses can be estimated by longitudinally decomposing the RFQ
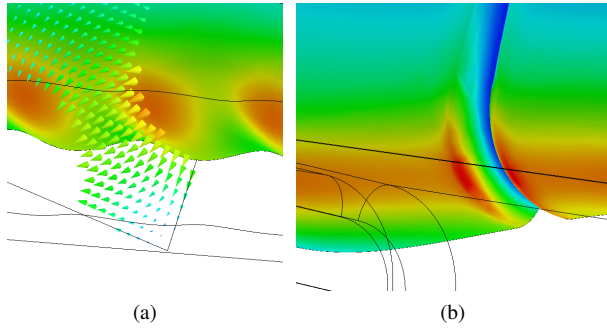
Figure 2: Surface and transverse electric field (a) at the vane and (b) at the module gap with a maximum of $E_s = 39.1$ MV/m.
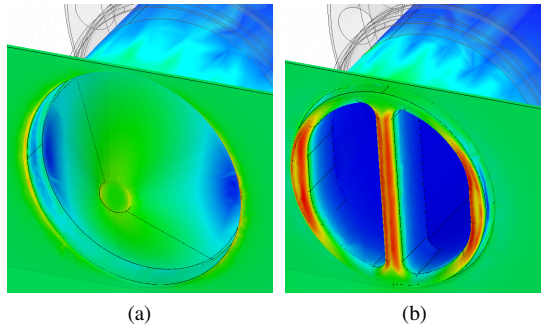

Figure 3: Conical copper slug tuner (a) and vacuum pumping port (b) with surface current distribution.

into segments assuming that the stored energy over length W/L is constant along the RFQ. By individual simulation of the segments we obtain the loss factor $Q_{0,s}$ of each segment s. The capacitance over length $C'(z) = \mathrm{d}C/\mathrm{d}z$ changes along the accelerator due to the vane modulation and is interpolated by computing specific isolated cells. Using $P_0 = \omega_0 W/Q_0$ with $\omega_0 = 2\pi f_0$ and $W = CV^2/2$ for each segment we arrive at

$$P_0 = \frac{\omega_0 V^2}{2} \sum_s \frac{1}{Q_{0,s}} \int_{\text{Seg. } s} C'(z)\mathrm{d}z, \qquad (1)$$

which gives 64.1 kW for the nominal voltage $V = 35$ kV. The approach allows to compute capacitance and power loss of the entire accelerator without having to simulate the full model. For verification, we nevertheless conducted simulations of the full RFQ, from which we obtain 64.5 kW. The quantities are summarised in Table 2.

Table 2: Computed RF Quantities for 35 kV Nom. Voltage

Loss factor	Q_0	6000	
Capacitance	C'	125	pF/m
Stored energy	W	82	mJ
RF power loss	P_0	64.5	kW
Max. surface field	E_s	39.1	MV/m

The PIXE RFQ features one single input power coupler (Fig. 4), which replaces one of the pumping ports in the

second module. It is a coaxial magnetic loop coupler, which is over-coupled by design with the coupling coefficient of $Q_0/Q_E = 1.25$ as safety margin. The coupler will be mounted on a rotatable flange which allows for reducing the external Q_E to achieve reflection-free coupling after assembly.
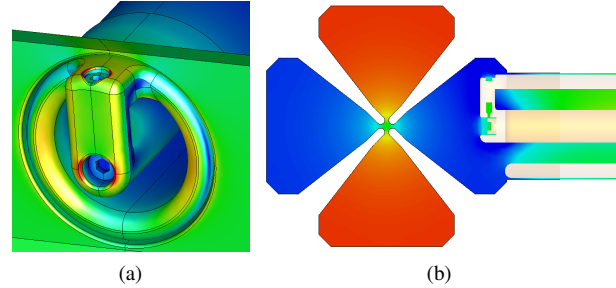

Figure 4: Input power coupler with coaxial loop geometry: (a) surface current distribution and (b) transverse section with z-component of magnetic field.

THERMAL SIMULATION

Due to the RF power loss at the inner surface of the RFQ, the temperature of the structure increases and it is deformed by thermal expansion, which shifts the resonant frequency of the cavity. Thermal simulations are conducted to study the dependence of the shift Δf on duty cycle d and cooling water temperature θ_w, utilising software [6–8].

The heat transfer coefficients depend on the water speed v_w: For $v_w = 2$ m/s, values of 7500 and 7310 W/m^2/K are assumed for the ∅5 and ∅8 cooling channels respectively, while for $v_w = 1$ m/s both channels have 3900 W/m^2/K. Additionally, the copper-to-air convection is estimated with 10 W/m^2/K.

Distributions of heat load, temperature and deformation are shown in Fig. 5. Figure 5c demonstrates that if the RFQ is heated, the tank size and thus the inductance L increases. Due to the temperature difference between vane and tank however, the vane tips move closer towards the beam axis, increasing capacitance C. Both effects reduce the resonance frequency, since $\partial f/f = -(\partial C/C + \partial L/L)/2$ holds for a resonant LC circuit. The frequency shift within the considered domain is linear with respect to duty cycle and water temperature (Fig. 6). The sensitivities are $\partial f/\partial \theta_w = -13.3$ kHz/K and $\partial f/\partial d = -67.3$ kHz/% for a 2 m/s water flow speed. The latter changes only slightly when choosing a smaller (average) water flow speed, however it significantly reduces the requirements on the chiller in the cooling circuit. Therefore, a flow speed of 1 m/s is chosen.

Since the 3 dB bandwidth of the RFQ is only ±125 kHz, the RF source has to follow the shifting resonance frequency of the cavity to minimise reflected power. For the proposed range of operation (up to 2.5 % duty cycle), the effect on the particle transmission is minimal, as is shown at the end of the following section.
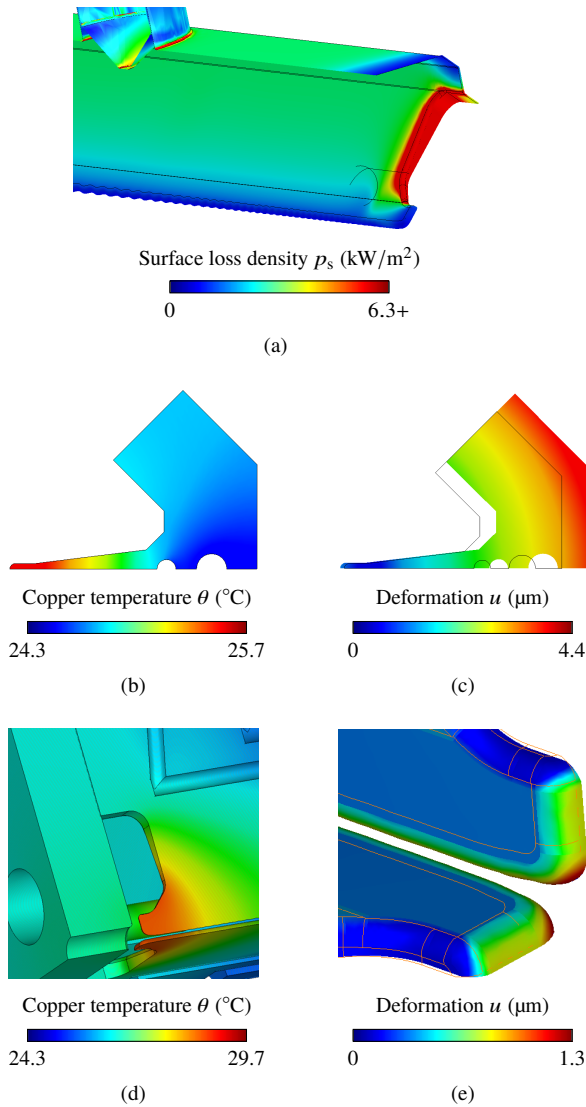
Surface loss density p_s (kW/m^2)

0   6.3+

(a)

Copper temperature θ (°C)

24.3   25.7

(b)

Deformation u (µm)

0   4.4

(c)

Copper temperature θ (°C)

24.3   29.7

(d)

Deformation u (µm)

0   1.3

(e)

Figure 5: Thermal simulation results for nominal parameters (2.5 % duty cycle, $\theta_w = 22$ °C, $v_w = 1$ m/s). (a) Power loss p_s on cavity surface. (b) temperature θ and (c) deformation u of the octant-symmetric cross section; (d), (e) respective results around the vane nose.

1D PARTICLE TRACKING

To validate computed RF fields, particle tracking is performed to simulate the effect of these fields on the longitudinal beam dynamics. Phase and energy of the particles are calculated in the RF field. The particles are moving with $x = y = 0$ along the z-axis of the RFQ. The initial phase spreads from 0 to 2π and the initial energy is 20 keV.

Figure 7 shows the computed phase and energy along the beam axis. As the particle velocity changes significantly over the length of the RFQ, we define the phase from the vane modulation:

$$\Delta\phi_P(t) = \phi_{0,p} + \omega_0 t - \pi \int_{z_0}^{z_P(t)} \frac{\mathrm{d}z}{\mathcal{L}(z)}, \qquad (2)$$

where $z_p(t)$ is the computed trajectory of particle p and $\mathcal{L}(z)$ is a continuous function interpolated from the lengths of the
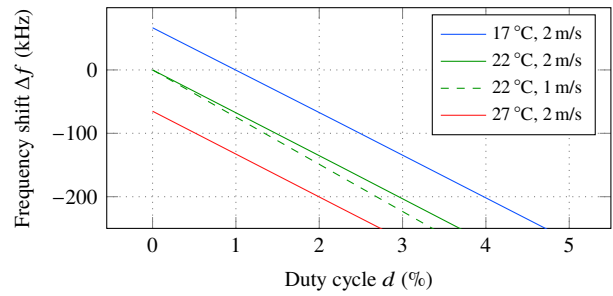

Figure 6: Dependence of the frequency shift of the RFQ cavity subject to RF losses in on the duty cycle.

RFQ cells. The transmission T is defined as the percentage of input particles that are bunched and accelerated to 2 MeV. Because of the peculiar setup solely considering longitudinal beam dynamics, $T = 23$ % of particles are captured within the first 10 cm of the RFQ. As mentioned in the previous section, the effect of a shifting RF frequency within the limits of Fig. 6 is minimal, which is demonstrated in Fig. 8.
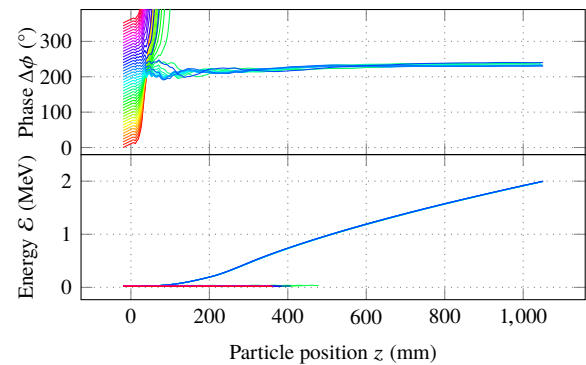

Figure 7: Phase and energy of the tracked particles along the RFQ. The color indicates the start phase of the particle relative to the RF field.
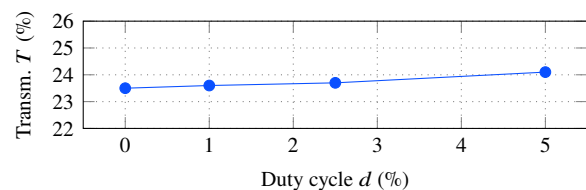

Figure 8: Transmission of a beam through the RFQ as a function of the duty cycle.

CONCLUSION

The RF design of the PIXE RFQ linac has been conducted including cavity geometry, tuners, pumping ports, and power coupler. The thermal expansion and resulting resonant frequency shift due to RF power dissipation has been studied to yield the requirements on the cooling circuit. Further, first results of particle tracking through the RF field have been presented. It has been shown, that the frequency shift due thermal expansion has little effect on the beam dynamics.

Proton and Ion Accelerators and Applications

RFQs

REFERENCES

[1] S. A. E. Johansson *et al.*, *Particle-induced X-ray emission spectrometry (PIXE)*, vol. 133, John Wiley & Sons, 1995

[2] M. Vretenar *et al.*, "High-frequency compact RFQs for medical and industrial applications," in *Proc. 28th Linear Accelerator Conf. (LINAC'16)*, East Lansing, MI, USA, 2016. `doi:10.18429/JACoW-LINAC2016-TH1A06`

[3] L. Giuntini *et al.*, "MACHINA: movable accelerator for cultural heritage in-situ non-destructive analysis," in *Proc. 16th International Conference on Nuclear Microprobe Technology and Applications (ICNMTA'18)*, Guilford, Surrey, England, 2018

[4] A. Lombardi *et al.*, "Beam dynamics in a high frequency RFQ," in *Proc. 6th Int. Particle Accelerator Conf. (IPAC'15)*, Richmond, VA, USA, 2015. `doi:10.18429/JACoW-IPAC2015-MOPJE042`

[5] B. Koubek *et al.*, "Tuning of the CERN 750 MHz RFQ for medical applications," in *Proc. 28th Linear Accelerator Conf. (LINAC'16)*, East Lansing, MI, USA, 2016. `doi:10.18429/JACoW-LINAC2016-THOP09`

[6] Computer Simulation Technology, *CST Studio Suite 2018*

[7] ANSYS. Electromagnetics Suite, *Release 17.2*

[8] ANSYS. Mechanical, *Release 17.2*